

Origin of size effect on superconductivity in $(R_{0.8}Pr_{0.2})Ba_2Cu_3O_7$ studied by soft X-ray absorption spectroscopy

J.M. Chen ^{a,*}, P. Nachimuthu ^a, J.Y. Lin ^b, I.P. Hong ^c, C.F. Chang ^c, H.D. Yang ^c

^a Synchrotron Radiation Research Center (SRRC), Hsinchu, Taiwan, ROC

^b Department of Physics, National Chiao Tung University, Hsinchu, Taiwan, ROC

^c Department of Physics, National Sun Yat-Sen University, Kaohsiung, Taiwan, ROC

Received 19 September 2000; in final form 18 December 2000

Abstract

O K-edge X-ray absorption near-edge structure (XANES) spectroscopy of $(R_{0.8}Pr_{0.2})Ba_2Cu_3O_7$ ($R = Y, Tm, Dy, Gd, Eu$ and Sm) has been performed to investigate the dependence of hole distribution on ionic size of the R^{3+} ions. Near the O 1s absorption edge, pre-peaks at ~ 527.8 and ~ 528.5 eV are assigned to transitions into O 2p hole states located in the CuO_3 ribbons and CuO_2 planes, respectively. As deduced from O K-edge X-ray absorption spectra, the hole concentrations in the CuO_2 planes decrease monotonically with increasing ionic size of the rare-earth elements. The present XANES results clearly demonstrate that the suppression of superconductivity in $(R_{1-x}Pr_x)Ba_2Cu_3O_7$ with ionic radius of the R^{3+} ions results predominantly from the hole-depletion effect. © 2001 Elsevier Science B.V. All rights reserved.

1. Introduction

It has been well established that chemical substitution of Y in $YBa_2Cu_3O_7$ by rare earth elements R ($R = Nd, Sm, Eu, Gd, Dy, Ho, Er, Tm, Yb,$ and Lu) neither affects its superconducting properties nor significantly changes the corresponding superconducting transition temperature (T_c) of ~ 92 K [1]. However, for $R = Pr$, superconductivity is completely suppressed. Furthermore, the Pr moments in $PrBa_2Cu_3O_7$ order antiferromagnetically with a Néel temperature of 17 K [2]. This is in contrast to the other $RBa_2Cu_3O_7$

compounds in which the rare-earth moments order at lower temperature (< 2.5 K). The absence of superconductivity in $PrBa_2Cu_3O_7$ has long remained a remarkable puzzle. Although much experimental and theoretical work has been undertaken, the mechanism of superconductivity suppression in $PrBa_2Cu_3O_7$ is still the subject of controversial discussion [3]. More recently, superconductivity of $PrBa_2Cu_3O_7$ has been reported. However, these reports have met with considerable scepticism due to the lack of reproducibility of data and an anomalous long c axis for the structure of $PrBa_2Cu_3O_7$ [4,5].

The substitution of Y by Pr in $(Y_{1-x}Pr_x)Ba_2Cu_3O_7$ leads to a significant decrease in T_c with superconductivity disappearing at $x \geq 0.55$ [6]. Several possible mechanisms have been proposed

*Corresponding author. Fax: +866-3-5789816.

E-mail address: jmchen@srcc.gov.tw (J.M. Chen).

to explain the suppression of T_c by Pr doping in $(Y_{1-x}Pr_x)Ba_2Cu_3O_7$. These models include hole filling [7], hole localization [8], percolation [9], magnetic pair-breaking [7], disorder on Ba sites [10], hole transfer from planes to chains [11], etc. However, none of these models allow a consistent interpretation of all the experimental results. For example, in the hole-filling model, the valence of the Pr ion is assumed to be 4+. Thus, upon substituting Pr into the $(Y_{1-x}Pr_x)Ba_2Cu_3O_7$ system, some of the holes will be annihilated due to the replacement of trivalent Y ions with tetravalent Pr ions. This model implies that the Pr-induced T_c suppression originates from a reduction in the number of holes in the CuO_2 planes. The hole-filling model is able to account for the lack of metallic property in $PrBa_2Cu_3O_7$ and account for the Ca-induced recovery of superconductivity in $(Pr_{0.5}Ca_{0.5})Ba_2Cu_3O_7$ thin films [12]. The hole-filling model was also supported by several experiments which include nuclear magnetic resonance [13], neutron diffraction [14], Hall effect [15], thermoelectric power [16], heat capacity [17], magnetic susceptibility [15,17], and chemical substitution [7]. However, this model was criticized in view of experimental results based on valence-band resonant photoemission [18], X-ray absorption spectroscopy [19], and Raman spectroscopy [20] which were interpreted in terms of the simple Pr^{3+} ion. Thus, these results ruled out hole filling as an explanation for the suppression of superconductivity in $(R_{1-x}Pr_x)Ba_2Cu_3O_7$ by Pr doping.

It has been observed that the depression rate of T_c by Pr doping is R-radius dependent in $(R_{1-x}Pr_x)Ba_2Cu_3O_7$ with fixed x . The smaller the atomic number of rare-earth elements in host compounds the greater the decrease in T_c [21]. The magnetic ordering temperature (T_N) of Pr ions [22] and the normal state resistivity [23] in $(R_{1-x}Pr_x)Ba_2Cu_3O_7$ are also R ion size dependent. Recently, it was found that substituting Sr for Ba in $(R_{1-x}Pr_x)BaSrCu_3O_7$ mitigated the T_c suppression, indicating that a similar ionic size effect occurs at Ba sites [24].

Although the physical properties of $(R_{1-x}Pr_x)Ba_2Cu_3O_7$ with various rare-earth elements have been widely studied [23,25], no investigations into the electronic structure of these compounds have

been performed. It is therefore of great interest to investigate the variations of electronic structure related to the ionic size of R-site elements in $(R_{1-x}Pr_x)Ba_2Cu_3O_7$ with fixed x . It is well known that hole states near the Fermi level play a pivotal role for superconductivity in the p-type cuprate superconductors. Thus, a knowledge of the electronic structure near the Fermi level of cuprate compounds is an important step toward unveiling the mechanism of superconductivity. X-ray absorption near-edge structure (XANES) using synchrotron radiation serves as a powerful tool for the investigation of the unoccupied electronic states in high- T_c superconductors. In this study, O K-edge X-ray absorption measurements for $(R_{0.8}Pr_{0.2})Ba_2Cu_3O_7$ ($R = Y, Tm, Dy, Gd, Eu$ and Sm) were performed in an attempt to delineate the dependence of the hole distribution on the ionic size of the R^{3+} ions.

2. Experiments

The detailed procedures for the preparation of samples were reported elsewhere [26], so only pertinent details are given here. The $(R_{0.8}Pr_{0.2})Ba_2Cu_3O_7$ samples ($R = Y, Tm, Dy, Gd, Eu$ and Sm) were prepared by solid-state reaction. Appropriate amounts of high-purity $R_2O_3, Pr_6O_{11}, BaCO_3$, and CuO were mixed and calcinated in air at $950^\circ C$ for 24 h. The reacted samples were pressed into pellets and heated in air at $950^\circ C$ for 24 h. This process was repeated several times. These pellets were then heated in flowing 100% O_2 at $950^\circ C$ for 48 h, followed by an additional annealing at $450^\circ C$ for 12 h. All the samples were prepared at the same time in the same furnace to ensure the same sample history. The oxygen contents for all the samples were determined by the isometric method. X-ray powder diffraction patterns showed that all the samples were single phase corresponding to the orthorhombic structure. The homogeneity of each sample was also checked by the Messiner effect. Electrical resistivity measurements were performed on rectangular specimens cut from sintered pellets employing the standard four-probe method with silver paint contacts attached to electrical leads.

X-ray absorption measurements for all the samples were performed at the 6 m high-energy spherical grating monochromator (HSGM) beamline of the Synchrotron Radiation Research Center (SRRC) in Taiwan with an electron beam energy of 1.5 GeV. X-ray absorption spectra recorded by the X-ray fluorescence-yield method were measured using a microchannel plate (MCP) detector. This detector is composed of a dual set of MCPs with an electrically isolated grid mounted in front of them. The X-ray fluorescence-yield measurement is strictly bulk sensitive with a probing depth of thousands of angstroms. During the X-ray fluorescence-yield measurements, the grid was set to a voltage of 100 V while the front of the MCPs was set to -2000 V and the rear to -200 V. The negative MCP bias was applied to expel electrons, while the positive grid bias ensured that no positive ions were detected. The MCP detector was oriented parallel to the sample surface. Photons were incident at an angle of 45° with respect to the sample normal. The incident photon intensity (I_0) was measured simultaneously using a Ni mesh located after the exit slit of the monochromator. All the absorption spectra were normalized to (I_0). The photon energies were calibrated using the known O K-edge absorption peaks of CuO. The energy resolution of the monochromator was set to ~ 0.22 eV for the O K-edge X-ray absorption measurements. All the measurements were carried out at room temperature.

3. Results and discussion

The electrical resistivity $\rho(T)$ as a function of temperature for the series of $(R_{0.8}Pr_{0.2})Ba_2Cu_3O_7$ samples ($R = Y, Tm, Dy, Gd, Eu$ and Sm) is reproduced in Fig. 1. The resistivity curves and corresponding T_c values are in excellent agreement with earlier reports [27]. The resultant T_c values as a function of ionic radius of rare-earth elements are displayed in Fig. 2. As shown, a nearly linear relationship between T_c and the ionic radius of R-site elements in $(R_{0.8}Pr_{0.2})Ba_2Cu_3O_7$ is obtained. The chemical substitution of various R elements into the $(R_{0.8}Pr_{0.2})Ba_2Cu_3O_7$ system leads to a monotonical decrease of the superconducting

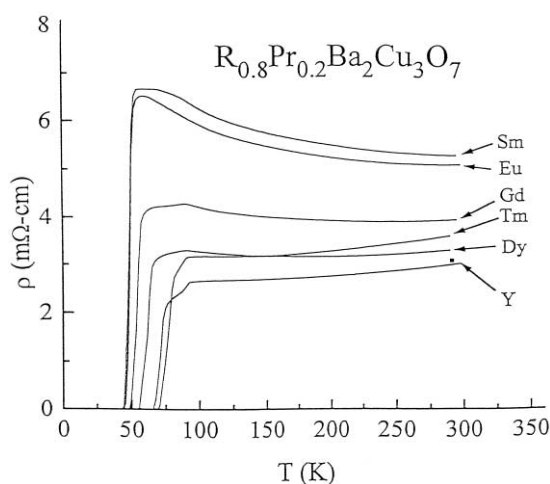


Fig. 1. Temperature dependence of the electrical resistivity $\rho(T)$ of $(R_{0.8}Pr_{0.2})Ba_2Cu_3O_7$ ($R = Y, Tm, Dy, Gd, Eu$ and Sm).

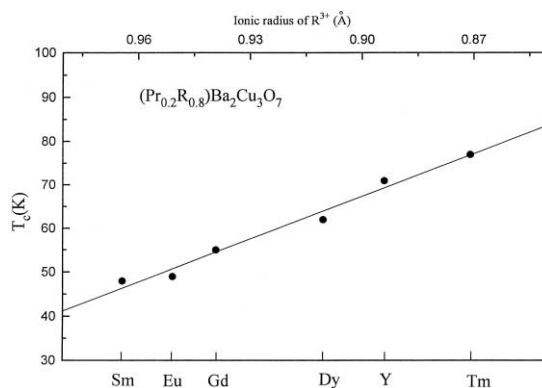


Fig. 2. T_c as a function of ionic radius of R-site elements in $(R_{0.8}Pr_{0.2})Ba_2Cu_3O_7$ ($R = Y, Tm, Dy, Gd, Eu$ and Sm).

transition temperature with increasing ionic size of the R^{3+} ions from $T_c \sim 80$ K for $R = Tm$ to $T_c \sim 48$ K for $R = Sm$. In other words, for R ions with a larger ionic radius in $(R_{0.8}Pr_{0.2})Ba_2Cu_3O_7$, a stronger T_c suppression by doping with the same Pr concentration is observed. These results are in accordance with the earlier reports [21,23].

In Fig. 3, O K-edge X-ray absorption spectra of $(R_{0.8}Pr_{0.2})Ba_2Cu_3O_7$ for $R = Y, Tm, Dy, Gd, Eu$ and Sm are shown in the energy range 524–546 eV obtained by a bulk-sensitive X-ray fluorescence-yield technique. The predominant features in the O 1s X-ray absorption spectra of $(R_{0.8}Pr_{0.2})$

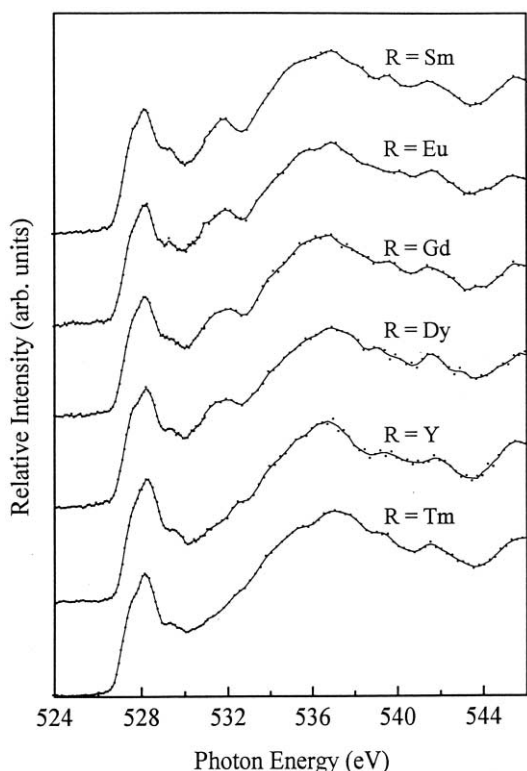


Fig. 3. O K-edge X-ray absorption spectra for a series of $(R_{0.8}Pr_{0.2})Ba_2Cu_3O_{7-\delta}$ compounds ($R = Y, Tm, Dy, Gd, Eu$ and Sm). The O K-edge X-ray absorption spectra for these compounds were normalized to the intensity in the energy of 535–555 eV with respect to the number of O atoms per unit cell.

$Ba_2Cu_3O_7$ are two distinct pre-peaks at ~ 528.5 and ~ 529.5 eV with a shoulder at ~ 527.8 eV, and a broad peak at ~ 537 eV. The low-energy pre-peaks with energy below 532 eV are ascribed to excitations of the O 1s electrons to hole states with major O 2p character. The enhanced peaks above 535 eV in $(R_{0.8}Pr_{0.2})Ba_2Cu_3O_{7-\delta}$ may be related to unoccupied states originating from the Ba 4d, Cu 4s or Cu 4p states hybridized with O 2p states [8]. As shown, the X-ray absorption spectra with energy beyond 535 eV for all the samples under study exhibit very similar features. Thus, the O K-edge X-ray absorption spectra for various compounds in Fig. 1 were normalized to the intensity in the energy range between 535 and 555 eV with respect to the number of O atoms per unit cell, providing the absolute intensities of the pre-peaks of cuprate compounds.

The crystal structure of $YBa_2Cu_3O_7$ is composed of two $Cu(2)O(2)O(3)$ layers separated by a Y plane. The unit of CuO_2 and Y planes are separated by a CuO_3 ribbon consisting of a $BaO(4)$ plane, a $Cu(1)O(1)$ chain along the b axis, and another $BaO(4)$ plane. Therefore, there exist four nonequivalent oxygen sites in $YBa_2Cu_3O_7$, O(2) and O(3) within the $Cu(2)O_2$ layers, O(4) in the BaO planes, and O(1) in the $Cu(1)O$ chains. The observed multiple pre-peaks in O K-edge absorption spectra shown in Fig. 3 are due to chemical shifts originating from the influence of charges on the oxygen sites and the site-specific neighbourhood. Based on polarization-dependent O K-edge X-ray absorption measurements in $(Y_{1-x}Pr_x)Ba_2Cu_3O_{7-\delta}$ single crystals, the pre-peaks at ~ 527.8 eV are assigned to transitions into O 2p hole states in the CuO_3 ribbons. The high-energy pre-peak at ~ 528.5 eV is ascribed to transitions into O 2p hole states within the CuO_2 planes [28].

Compounds of the type $(R_{0.8}Pr_{0.2})Ba_2Cu_3O_{7-\delta}$ ($R = Tm, Dy, Gd, Eu$ and Sm) are isomorphic with orthorhombic $YBa_2Cu_3O_{7-\delta}$ (space group: $Pmmm$) and $(Y_{0.8}Pr_{0.2})Ba_2Cu_3O_{7-\delta}$. As shown in Fig. 3, the O 1s near edge of $(R_{0.8}Pr_{0.2})Ba_2Cu_3O_{7-\delta}$ exhibits similar features as observed in $YBa_2Cu_3O_{7-\delta}$ and $(Y_{0.8}Pr_{0.2})Ba_2Cu_3O_{7-\delta}$ with $\delta = 0$ [28]. We therefore adopt the same assignment scheme for the O K-edge X-ray absorption spectra of $(R_{0.8}Pr_{0.2})Ba_2Cu_3O_{7-\delta}$ ($R = Tm, Dy, Gd, Eu$ and Sm). The high-energy pre-peak at ~ 528.5 eV is attributed to photoexcitations of O 1s electrons to O 2p hole states in the CuO_2 planes. The low-energy pre-peaks at ~ 527.8 eV are due to the superposition of O 2p hole states in the apical oxygen sites and the CuO chains. The absorption peak at ~ 529.5 eV is ascribed to transitions into the empty upper Hubbard band (UHB) with major Cu 3d character [28]. This kind of pre-edge structure is due to hybridization in the ground state of the Cu $3d^9$ and Cu $3d^{10}L$ states, where L is a ligand hole from the O 2p band.

In order to investigate the variations of hole states among different oxygen sites as a function of the ionic size of R-site elements, these pre-edge features shown in Fig. 3 were analysed by fitting each spectrum with Gaussian functions. It was found that the peak widths obtained from the

fitting were almost constant for a particular pre-peak over a series. These peak widths were averaged over a series for particular pre-peak. The resultant peak widths were then fixed for the final fitting. In Fig. 4 the relative intensity of each pre-peak is plotted as a function of R-site elements in $(R_{0.8}Pr_{0.2})Ba_2Cu_3O_7$ ($R = Y, Tm, Dy, Gd, Eu$ and Sm). As noted from Figs. 4a and 4b, the hole content from the CuO_2 planes decreases monotonically with increasing ionic size of the R^{3+} ions, while that from the apical oxygen sites and the CuO chains is almost kept constant. This result clearly reveals that the larger ionic radius of R-site elements in the host $(R_{1-x}Pr_x)Ba_2Cu_3O_7$ compounds leads to the greater reduction in hole concentration in the CuO_2 planes when the various rare-earth elements are substituted into the R sites. In addition, as shown in Fig. 4c, the pre-peak at

~ 529.5 eV originating from the UHB shows a monotonic increase in spectral weight as the ionic radius of R-site elements increases. This change is due to the spectral weight transfer of states from the UHB to doping-induced hole states near the Fermi level. Similar behaviour has also been observed in O 1s X-ray absorption spectra of other p-type cuprate superconductors [28,29].

It has been proposed by Fehrenbacher and Rice (FR) that, in $PrBa_2Cu_3O_7$, there exists a hybridized Pr 4f–O2 p_π electronic state [30]. This hybridized state is competitive in energy to the hole states in the CuO_2 planes. The FR model proposed hole depletion in the CuO_2 planes with Pr doping, because of transfer of the holes from the CuO_2 planes into the FR state which binds doped holes to the Pr sites. The observed decrease in T_c with increasing hydrostatic pressure in $(Y_{1-x}Pr_x)Ba_2Cu_3O_7$ system supports the FR model [31]. The FR model resolves the controversy on the different valence values of the Pr ion obtained from different measurements. However, this model cannot account for the R-radius dependence on the T_c suppression in $(R_{1-x}Pr_x)Ba_2Cu_3O_7$.

Based on the concept of FR states, Liechtenstein and Mazin (LM) calculated the electronic structure of $(R_{1-x}Pr_x)Ba_2Cu_3O_7$ using ab initio local density approximation plus Hubbard including Coulomb correlation in the Pr 4f shell [32]. They found that, in $PrBa_2Cu_3O_7$, there forms an additional hole-depleting band which crosses the Fermi level and consequently grabs the mobile holes from the CuO_2 band. In addition, the LM model demonstrated that the position of the f band of the rare-earth element R can affect the rate of hole depletion from the CuO_2 planes and lead to the observed ionic-size effect in $(R_{1-x}Pr_x)Ba_2Cu_3O_7$ [32].

It was argued that the energy of p–f hybridized state may depend on the extent of the Pr 4f–O 2p hybridization. Recently, Cao et al. [33] suggested that smaller ions on Y or Ba sites decrease the extent of Pr 4f–O 2p hybridization, resulting in the decrease of the position of the hole-depletion band relative to the hole states in the CuO_2 planes. Thus, for smaller R^{3+} ions in $(R_{1-x}Pr_x)Ba_2Cu_3O_7$, the resultant hole depletion is mitigated and the hole content in the CuO_2 plane is higher.

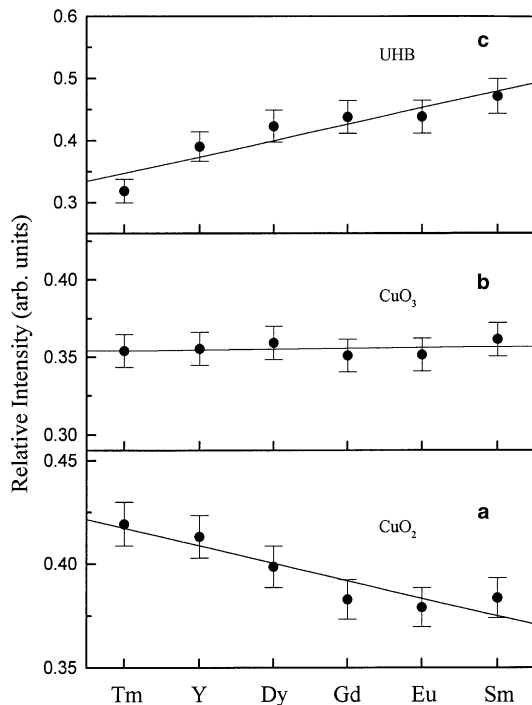


Fig. 4. R-dependence of the relative intensity of hole states in $(R_{0.8}Pr_{0.2})Ba_2Cu_3O_7$ ($R = Y, Tm, Dy, Gd, Eu$ and Sm) on the oxygen sites originating from the: (a) CuO_2 planes; (b) CuO_3 ribbons; (c) UHB. The solid curves are drawn as a guide to the eye.

Recently, based on polarization-dependent O K-edge X-ray absorption measurements in detwinned $(Y_{1-x}Pr_x)Ba_2Cu_3O_7$ single crystals by Merz et al. [28], their result is consistent with approaches based on Pr 4f–O 2p $_{\pi}$ hybridization and consequently rules out a number of theoretical models, such as hole filling and charge transfer between the planes and the chains. However, their result falls between the localized model of FR and the band model of LM and therefore it is difficult to prove which model is valid.

As shown in Figs. 3 and 4, the monotonic reduction of hole concentrations in the CuO_2 planes with increasing ionic radius of the R^{3+} ions in $(R_{0.8}Pr_{0.2})Ba_2Cu_3O_7$ provides clear evidence in support of hole-depletion model proposed by Liechtenstein and Mazin [32]. From the Hall measurements in $(R_{0.8}Pr_{0.2})Ba_2Cu_3O_7$ by Chen et al. [23], it was found that, at a constant temperature, the Hall number (mobile hole) decreases roughly linearly with increasing R^{3+} ionic radius, consistent with the present observation. Ramesh et al. [34], reported that, based on a calculation of the bond-valence sums for $RBa_2Cu_3O_7$, the valence of the in-plane copper increases with decreasing radius of R elements. This implies an increase of hole concentrations in the CuO_2 plane with decreasing ionic radius of the R^{3+} ions.

It has been experimentally shown that the concentration of O 2p holes in the CuO_2 planes is strongly correlated with T_c in the p-type cuprate superconductors. Accordingly, the T_c value in $(R_{0.8}Pr_{0.2})Ba_2Cu_3O_7$ decrease with increasing ionic radius of the R^{3+} ions. Our experimental results therefore clearly reveal that the dependence of the superconductivity quenching in $(R_{0.8}Pr_{0.2})Ba_2Cu_3O_7$ on the ionic radius of the R element results predominantly from hole depletion [35].

4. Conclusion

We present the first report of hole distribution related to ionic size effect in $(R_{0.8}Pr_{0.2})Ba_2Cu_3O_7$ ($R = Y, Tm, Dy, Gd, Eu$ and Sm) using O K-edge X-ray absorption spectroscopy. As deduced from O K-edge X-ray absorption spectra, the hole concentrations in the CuO_2 planes decrease

monotonically in $(R_{0.8}Pr_{0.2})Ba_2Cu_3O_7$ with increasing ionic size of the R^{3+} ions, consistent with the hole-depletion model based on the Pr 4f–O 2p $_{\pi}$ hybridization. The present XANES results clearly demonstrate that the superconductivity suppression in $(R_{1-x}Pr_x)Ba_2Cu_3O_7$ with ionic radius of R^{3+} ions arises predominantly from the hole-depletion effect.

Acknowledgements

We thank SRRC staff for their technical support. This research is financially supported by SRRC and National Science Council of the Republic of China under grant numbers NSC 86-2613-M-213-010 and NSC 89-2113-M-213-002.

References

- [1] P.H. Hor, R.L. Meng, Y.Q. Wang, L. Gao, Z.L. Huang, J. Bechtold, K. Forster, C.W. Chu, Phys. Rev. Lett. 58 (1987) 1891.
- [2] K. Nehrke, M.W. Pieper, Phys. Rev. Lett. 76 (1996) 1936.
- [3] H.B. Radousky, J. Mater. Res. 7 (1992) 1917 (and references therein).
- [4] Z. Zou, J. Ye, K. Oka, Y. Nishihara, Phys. Rev. Lett. 80 (1998) 1074.
- [5] V.N. Narozhnyi, S.L. Drechsler, Phys. Rev. Lett. 82 (1999) 461.
- [6] L. Soderholm, K. Zhang, D.G. Hinks, M.A. Beno, J.D. Jorgensen, C.U. Segre, I.K. Schuller, Nature (London) 328 (1987) 604.
- [7] J.J. Neumeier, T. Bjornholm, M.B. Maple, I.K. Schuller, Phys. Rev. Lett. 63 (1989) 2516.
- [8] J. Fink, N. Nücker, H. Romberg, M. Alexander, M.B. Maple, J.J. Neumeier, J.W. Allen, Phys. Rev. B 42 (1990) 4823.
- [9] C. Infante, M.K. El Mousky, R. Dayal, M. Husain, S.A. Siddiqi, P. Ganguly, Physica C 167 (1990) 640.
- [10] H.A. Blackstead, J.D. Dow, Phys. Rev. B 50 (1994) 10350.
- [11] D. Khomskii, J. Supercond. 6 (1993) 69.
- [12] D.P. Norton, D.H. Lowndes, B.C. Sales, J.D. Budai, B.C. Chakoumakos, H.R. Kerchner, Phys. Rev. Lett. 66 (1991) 1537.
- [13] A.P. Reyes, D.E. MacLaughlin, M. Takigawa, P.C. Hammel, R.H. Heffner, J.D. Thompson, J.E. Crow, Phys. Rev. B 43 (1991) 2989.
- [14] M. Guillaume, P. Allenspach, J. Mesot, B. Roessli, U. Staub, P. Fisher, A. Furrer, Z. Phys. B 90 (1993) 13.
- [15] A. Matsuda, K. Kinoshita, T. Ishii, H. Shibata, T. Wantabe, T. Yanada, Phys. Rev. B 38 (1988) 2910.

- [16] A.P. Gonclaves, I.C. Santos, E.B. Lopes, R.T. Henriques, M. Almeida, M.O. Figueiredo, *Phys. Rev. B* 37 (1988) 7476.
- [17] A. Kebede, C.S. Jee, J. Schwegler, J.E. Crow, T. Mihalisin, G.H. Myer, R.E. Salomon, P. Schlottmann, M.V. Kuric, S.H. Bloom, R.P. Guertin, *Phys. Rev. B* 40 (1989) 4453.
- [18] J.S. Kang, J.W. Allen, Z.X. Shen, W.P. Ellis, J.J. Yeh, B.W. Lee, M.B. Maple, W.E. Spicer, I. Lindau, *J. Less Common Met.* 148 (1989) 121.
- [19] F.W. Lytle, G. van der Laan, R.B. Gregor, E.M. Larson, C.E. Violet, J. Wong, *Phys. Rev. B* 41 (1990) 8955.
- [20] H.J. Rosen, R.M. Macfarlane, E.M. Engler, V.Y. Lee, R.D. Jacowitz, *Phys. Rev. B* 38 (1988) 2460.
- [21] Y. Xu, W. Guan, *Solid State Commun.* 80 (1991) 105.
- [22] W.Y. Guan, Y.H. Xu, S.R. Sheen, Y.C. Chen, J.Y.T. Wei, H.F. Lai, M.K. Wu, J.C. Ho, *Phys. Rev. B* 49 (1994) 15993.
- [23] J.C. Chen, Y. Xu, M.K. Wu, W. Guan, *Phys. Rev. B* 53 (1996) 5839.
- [24] G. Cao, Y. Qian, Z. chen, X. Li, H. Wu, Y. Zhang, *Phys. Lett. A* 196 (1994) 263.
- [25] L.C. Tung, J.C. Chen, M.K. Wu, W. Guan, *Phys. Rev. B* 59 (1999) 4504.
- [26] H.D. Yang, P.F. Chen, C.R. Hsu, C.W. Lee, C.L. Li, C.C. Peng, *Phys. Rev. B* 43 (1989) 10568.
- [27] C.S. Jee, A. Kebede, D. Nichols, J.E. Crow, I. Mihalisin, G.H. Myer, I. Perez, R.E. Salomon, P. Schlottmann, *Solid State Commun.* 69 (1989) 379.
- [28] M. Merz, N. Nücker, E. Pellegrin, P. Schweiss, S. Schuppler, M. Kielwein, M. Knupfer, M.S. Golden, J. Fink, C.T. Chen, V. Chakarian, Y.U. Idzerda, A. Erb, *Phys. Rev. B* 55 (1997) 9160.
- [29] C.T. Chen, F. Sette, Y. Ma, M.S. Hybertsen, E.B. Stechel, W.M.C. Foulkes, M. Schluter, S.W. Cheong, A.S. Cooper, L.W. Rupp Jr., B. Batlogg, Y.L. Soo, Z.H. Ming, A. Krol, Y.H. Kao, *Phys. Rev. Lett.* 66 (1991) 104.
- [30] R. Fehrenbacher, T.M. Rice, *Phys. Rev. Lett.* 70 (1993) 3471.
- [31] J.J. Neumeier, M.B. Maple, M.S. Torikachcili, *Physica C* 156 (1998) 574.
- [32] A.I. Liechtenstein, I.I. Mazin, *Phys. Rev. Lett.* 74 (1995) 1000.
- [33] G. Cao, H. Song, Q. Zhang, *Physica C* 282–287 (1997) 761.
- [34] S. Ramesh, M.S. Hegde, *Physica C* 230 (1994) 135.
- [35] J.M. Chen, R.S. Liu, J.G. Lin, C.Y. Huang, J.C. Ho, *Phys. Rev. B* 55 (1997) 14586.